

Effects of pressure and temperature on the thermal conductivity of $\text{Sn}_2\text{P}_2\text{S}_6$

O. Andersson,¹ O. Chobal,² I. Rizak,³ V. Rizak,² and V. Sabadosh²

¹*Department of Physics, Umeå University, S-901 87 Umeå, Sweden*

²*Department of Solid State Electronics, Uzhhorod National University, 88000 Uzhhorod, Ukraine*

³*Department of Integrated Technologies of Aviation Manufacture, National Aerospace University of "KhAI," 61000 Kharkov, Ukraine*

(Received 9 February 2011; published 26 April 2011)

The thermal conductivity κ of the ferroelectric, paraelectric, and incommensurate phases of polycrystalline $\text{Sn}_2\text{P}_2\text{S}_6$ has been measured in the 0.1–0.7 GPa range. The thermal conductivity κ of the ferroelectric phase decreases with increasing pressure p . This unusual behavior, which is found in only a few other phases, is attributed to a negative Grüneisen parameter. The temperature T dependence of κ for the ferroelectric phase ($\kappa \sim T^{-1}$) is well described by the Debye model for κ , with three-phonon Umklapp scattering serving as the dominant scattering mechanism near and above the Debye temperature (~ 100 K) up to a few tenths of degrees below the ferro- to paraelectric phase transition, where $\kappa(T)$ gradually changes and becomes temperature independent upon further heating. The thermal conductivity of the paraelectric and incommensurate phases was temperature independent and indistinguishable. Possible causes for the unusually weak T dependence at high temperatures and implications of the p dependence of κ are discussed.

DOI: [10.1103/PhysRevB.83.134121](https://doi.org/10.1103/PhysRevB.83.134121)

PACS number(s): 44.10.+i, 77.80.-e, 72.20.-i, 63.20.Ry

I. INTRODUCTION

$\text{Sn}_2\text{P}_2\text{S}_6$ is an interesting material for both applications and fundamental science.^{1,2} $\text{Sn}_2\text{P}_2\text{S}_6$ has, for example, favorable optical, electro-optical and piezo-electrical properties that are interesting in photonics, and it belongs to a family of compounds that offers unique possibilities for studies of critical behavior. The pressure-temperature (p – T) phase diagram of $\text{Sn}_2\text{P}_2\text{S}_6$ reveals three phases at pressures below 1 GPa, and two of these are stable at atmospheric pressure. One is a ferroelectric phase, which is stable up to 337 K, where it transforms to a paraelectric phase via a second-order transition. The third phase is a high-pressure incommensurate phase and the phase lines between the three phases join in a triple point at ~ 0.19 GPa and ~ 294 K, which is also a Lifshitz point.³ In a recent study,⁴ we investigated the occurrence of critical points and used heat capacity and birefringence data to show that a (virtual) tricritical point and the Lifshitz point are located close to each other in the p – T phase diagram of $\text{Sn}_2\text{P}_2\text{S}_6$. Moreover, a similar analysis based on birefringence and spontaneous polarization data for $(\text{Pb}_y\text{Sn}_{1-y})_2\text{P}_2(\text{Se}_x\text{S}_{1-x})_6$ solid solutions suggests that these merge in a tricritical Lifshitz point in the p – T phase diagram of $(\text{Pb}_y\text{Sn}_{1-y})_2\text{P}_2(\text{Se}_x\text{S}_{1-x})_6$ with estimated coordinates $T = 225$ K, $p = 0.28$ GPa, $x = 0$, $y = 0.12$.⁴ That is, by varying the chemical composition, a tricritical Lifshitz point may be realized in the p – T – x – y diagram of $(\text{Pb}_y\text{Sn}_{1-y})_2\text{P}_2(\text{Se}_x\text{S}_{1-x})_6$.

The change of the type of the phase transition at a tricritical point is directly related to the renormalization of the conditions of the phonon-phonon interactions and anharmonic processes. Since the (virtual) tricritical point of $\text{Sn}_2\text{P}_2\text{S}_6$, which is estimated to occur at 0.23 GPa,⁴ is approached under high pressure, studies of anharmonic effects in $\text{Sn}_2\text{P}_2\text{S}_6$ under high pressure are of particular relevance. It is a well-known fact that the efficiency, or strength, of phonon-phonon scattering processes is related to the crystal anharmonicity, which is described by the Grüneisen parameter. Since phonon-phonon scattering is the main source of thermal resistivity in crystals at temperatures of order of and above the Debye temperature,

thermal-conductivity results provide valuable information concerning the crystal anharmonicity, which is a feature exploited here.

This work provides results for the high-pressure thermal conductivity κ for $\text{Sn}_2\text{P}_2\text{S}_6$, and establishes the changes of κ with pressure and temperature near the polycritical points. Besides the results describing the anharmonicity in the phases of $\text{Sn}_2\text{P}_2\text{S}_6$ via the Grüneisen parameter, they also show that κ for the ferroelectric phase becomes almost temperature independent prior to the paraelectric phase transition upon heating and that κ decreases with increasing pressure, both of which are unusual behaviors. The latter result has implications for the stability of the ferroelectric phase at high pressure, and indicates that it may collapse to an amorphous state upon pressurization at low temperatures where crystal-crystal transitions are kinetically hindered.⁵

II. EXPERIMENTAL DETAILS

The transient hot-wire method was used to simultaneously measure the thermal conductivity and the heat capacity per unit volume, where the latter results have already been reported.⁴ This method has previously been described in detail.^{6,7} Briefly, the hot-wire probe was a nickel wire, 0.1 mm in diameter and 40 mm long, placed horizontally in a ring of constant radius within a ~ 15 mm deep and 37 mm internal diameter Teflon container with a tight-sealing 5 mm Teflon cover. The Teflon cell is closely fitted inside a piston-cylinder-type apparatus of 45 mm internal diameter and the whole assembly is transferred to a hydraulic press that supplies the load. To determine κ the wire probe embedded in the sample (32 g of polycrystalline $\text{Sn}_2\text{P}_2\text{S}_6$ grown by the gas-transport reaction technique⁸ was heated by a 1.4 s duration electric pulse of almost constant power, yielding a temperature rise of about 3.5 K. The temperature rise of the wire as a function of time was calculated by using its electrical-resistance–temperature relation; that is, the wire works as both heater and sensor for the temperature rise. The analytical solution for the temperature

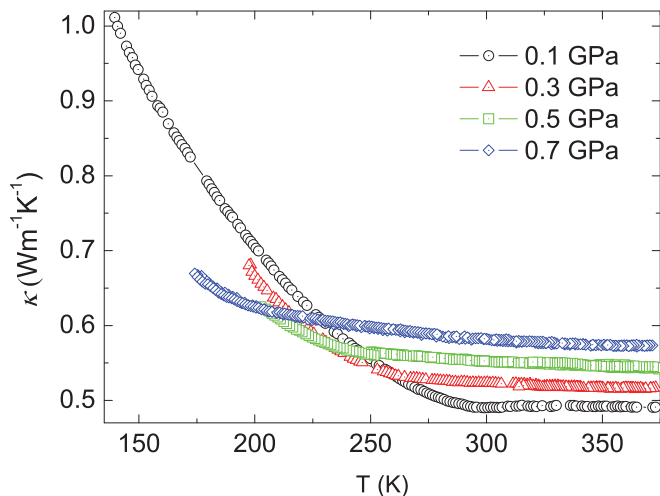


FIG. 1. (Color online) Thermal conductivity plotted against temperature for polycrystalline $\text{Sn}_2\text{P}_2\text{S}_6$, measured at the pressures indicated.

rise with time was fitted to the data for the hot-wire temperature rise with an inaccuracy of $\pm 2\%$ in κ .

The temperature of the piston-cylinder could be controlled by varying the power to an electrical resistance heater placed on the cylinder. For measurements below room temperature, the vessel was cooled using liquid nitrogen. The temperature of the specimen was measured by a Chromel-Alumel thermocouple, which had been previously calibrated against a commercially available silicon diode thermometer (stated accuracy ± 10 mK). The pressure fluctuation during isobaric measurements was less than ± 1 MPa.

III. RESULTS AND DISCUSSION

Figures 1 and 2 show results for κ of $\text{Sn}_2\text{P}_2\text{S}_6$ upon isobaric heating and isothermal pressurization. The isobaric data for κ show a gradual change from being strongly temperature dependent at low temperatures to almost constant at high temperatures, but there is no discernible discontinuous

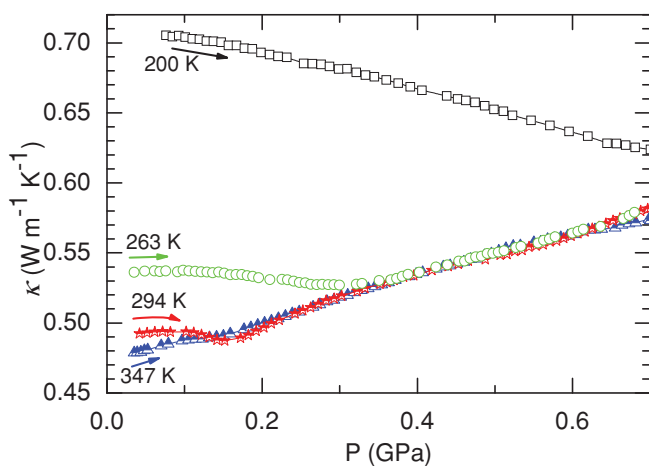


FIG. 2. (Color online) Thermal conductivity plotted against pressure for polycrystalline $\text{Sn}_2\text{P}_2\text{S}_6$, measured upon pressure increase at the temperatures indicated.

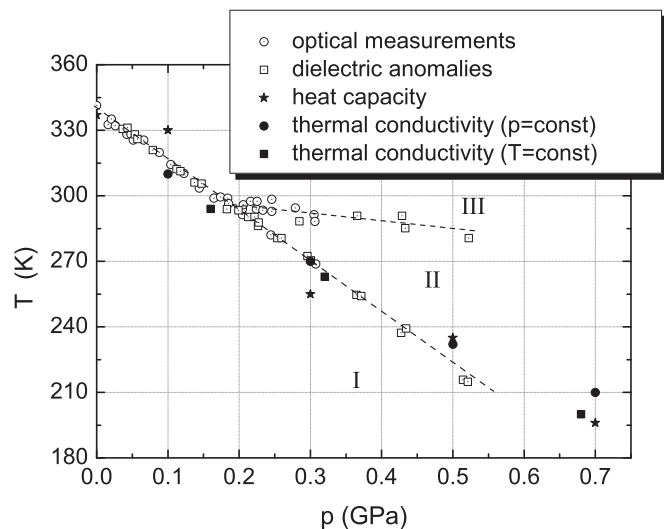


FIG. 3. p - T phase diagram of $\text{Sn}_2\text{P}_2\text{S}_6$ based on the data of Ref. 3 and results of heat capacity⁴ and thermal conductivity measurements. I is the ferroelectric phase, II is the incommensurate phase, and III is the paraelectric phase.

change, and this is typical for second-order transitions.⁹ The transition from the monoclinic ferroelectric phase (point group symmetry m) to the monoclinic paraelectric phase (point group symmetry $2/m$) is associated mainly with movement of the Sn atoms, whereas the $\text{P}_2\text{S}_6^{-4}$ units remain essentially unchanged (i.e. it is a displacive transition¹⁰). The gradual change in $\kappa(T)$ shifts to lower temperatures as the pressure is raised, which agrees with the negative slope of the T - p phase line between the ferroelectric phase and the paraelectric and incommensurate phases,³ as shown in Fig. 3, which suggests that it is a precursor of the phase transition (PT). PT features are also shown in $\kappa(p)$, which are more obvious as κ changes from decreasing in the ferroelectric phase to increasing in the paraelectric and incommensurate phases (Fig. 3). However, a transition between the latter phases cannot be distinguished in the data for κ . That is, κ of the paraelectric phase and κ of incommensurate phase have the same magnitude as well as the same temperature and pressure dependencies to within the precision of the method.

An analysis of the temperature dependence of κ for the ferroelectric phase well below the PT shows that it varies as $\kappa \sim T^{-n}$ with $n \approx 1$ for pressures in the 0.1–0.3 GPa range; namely, the same κ dependence as typically observed for crystals when three-phonon Umklapp scattering is the dominant phonon scattering mechanism.¹¹ In the vicinity and at temperatures above the PT, the behavior changes significantly and κ is only weakly decreasing with increasing temperature in the paraelectric phase of $\text{Sn}_2\text{P}_2\text{S}_6$. In fact, $\kappa(T)$ changes well below the PT. It becomes apparent at ~ 275 K upon heating at 0.1 GPa, where n strongly decreases upon further temperature increase. In the 275–300 K range, n is about 0.5 and κ even increases slightly ($n < 0$) before becoming weakly decreasing at ~ 313 K, which we have assigned to the ferroelectric to paraelectric PT. Due to the gradual change of $\kappa(T)$, it is difficult to determine unambiguously the PT coordinates from the $\kappa(T)$ data. However, the feature at ~ 313 K

agrees rather well with the phase line deduced from our data for $\kappa(p)$, which shows a more abrupt PT feature, as well as that obtained from dielectric data.³ It follows that the gradual change in $\kappa(T)$ toward almost constant κ starts a few tenths of degrees below the PT.

The weak temperature dependence of κ for the paraelectric phase and the ferroelectric phase at temperatures near the PT is typical for disordered phases such as orientationally disordered phases¹² and glasses. But there are also well-ordered crystalline phases showing a weak temperature dependence of κ or glasslike dependence; for example, ice clathrates,⁷ filled skutterudites,¹³ and two compounds of pyrochlore oxides: $\text{Cd}_2\text{Re}_2\text{O}_7$ and (ferroelectric) $\text{Cd}_2\text{Nb}_2\text{O}_7$.¹⁴ In the pyrochlore oxides, the glasslike behavior was attributed to strong coupling between acoustic modes and localized oscillations of the Cd ions. This explanation bears similarities with one of the models for the glasslike κ of ice clathrates and filled skutterudites, in which it is ascribed to resonant scattering caused by “rattler” modes of guest molecules that resides in host lattice cages. However, Koza *et al.*¹³ recently found this model incompatible with neutron spectroscopy and *ab initio* computational results for two cases of filled skutterudites. Instead, it was concluded that phonon scattering was caused by Umklapp processes (U processes) and possibly to some extent also by disorder due to partial filling of cages, which is in sharp contrast to the model of strong resonant scattering by guest “rattler” modes. In an analysis of κ for ice and ice clathrates, Dharma-wardana¹⁵ advocated a model that attributes the glasslike behavior for ice clathrates to their large number of atoms per unit cell. The numerous optical modes that arise were suggested to promote phonon-phonon scattering, which is a model that may be reconciled with the findings for filled skutterudites.¹³ But in the case of $\text{Sn}_2\text{P}_2\text{S}_6$, the number atoms in the unit cell do not change at the ferro- to paraelectric phase transition, and it is therefore an insufficient condition to explain the change of $\kappa(T)$. Moreover, all models which are based on phonon scattering by other phonons do not naturally give a weak temperature dependence of κ . One can conclude that the reason for the glasslike behavior observed in these different types of compounds cannot be regarded as established and may possibly have several different origins.

Considering the temperature dependence of κ for crystals in general, then the significant change in $\kappa(T)$ observed here is normally not associated with the displacive nature of the ferro- to paraelectric transition (i.e., the movement of the Sn atoms). But the transition is also accompanied by substantial changes in the acoustic and optical modes.¹⁶ Optical modes soften at temperatures well below the PT and dispersion relations of transverse and longitudinal acoustic modes flatten, which reduce the velocity of long-wave-vector phonons. The former effect can increase the participation of optical modes in phonon scattering and the latter diminishes the long-vector phonon contribution to κ . Moreover, we note that the transition has been referred to as a “mixed order-disorder/displacive transition”,¹⁶ and that an order-disorder component may be, at least partly, responsible for the changing $\kappa(T)$ behavior. Thus, one or a combination of these effects should be the cause of the change from $\kappa \sim T^{-1}$ to a low and almost temperature-independent κ , which is also further discussed in Ref. 17.

In order to discuss the size and temperature dependence of κ in more detail, we first consider the mechanisms of thermal conduction. It is known that the resistivity of $\text{Sn}_2\text{P}_2\text{S}_6$ crystals at room temperature is greater than 10^9 Ohm-cm¹⁸ and, therefore, the free electron contribution to κ is less than 1%, which is calculated from the Wiedemann-Franz relation. Thus, the heat is carried by phonons and models for phonon conduction can be used to describe $\kappa(T)$. In this case, we have employed an approximation for $\kappa(T)$ based on the relaxation time method and the Debye model of the phonon spectrum, which give¹¹

$$\kappa(T) = \frac{k}{2\pi^2 V_s} \left(\frac{k}{\hbar}\right)^3 T^3 \int_0^{\theta/T} \tau(x) \frac{x^4 e^x}{(e^x - 1)^2} dx, \quad x = \frac{\hbar\omega}{kT}, \quad (1)$$

where θ is the Debye temperature (~ 100 K), V_s is the mean velocity of sound, and $\tau(x)$ is the resultant relaxation time.

The inverse relaxation time $\tau^{-1}(x)$ is a sum of all relevant phonon scattering mechanisms:

$$\tau^{-1}(x) = \sum_i \tau_i^{-1}(x). \quad (2)$$

In a first attempt to describe the results, τ was calculated by taking into account scattering due to: (i) crystal grain boundaries, (ii) point defects (Rayleigh scattering), (iii) three phonon-phonon U processes, (iv) normal phonon processes, (v) resonance centers (resonance scattering), as well as (vi) other defects (assuming $\tau^{-1} \sim \omega$).¹¹ However, the analysis of the results of these calculations shows that $\kappa(T)$ of $\text{Sn}_2\text{P}_2\text{S}_6$, is well described by taking into account only U processes, phonon scattering at crystal boundaries, and point defects [i.e., processes (i)–(iii)], indicating that these are the dominant phonon scattering mechanisms. Thus, the expression for the inverse relaxation time for the phonons taking part in the heat transfer in $\text{Sn}_2\text{P}_2\text{S}_6$ crystals can be described by

$$\tau^{-1}(x) = A\omega^4 + B + DT\omega^2 e^{-C/T}, \quad (3)$$

where $C = -\theta/\beta$, and β , A , B , and D are constants. In Eq. (3), the first term describes Rayleigh scattering by point defects (small-size defects compared to the phonon wavelength), the second term B is associated with boundary scattering (i.e., it is determined by the crystal size), and the third term is due to phonon-phonon Umklapp scattering.^{11,19}

To determine the unknown parameters of the thermal conductivity function, we have used least-squares fitting; that is, the unknown parameters were determined by minimizing the expression

$$\sigma(A, B, C, D) = \sum_{i=1}^n [\kappa(A, B, C, D, T_i) - \kappa_{\text{expt}}(T_i)]^2, \quad (4)$$

where $\kappa_{\text{expt}}(T_i)$ are the experimental thermal conductivity values and $\kappa(A, B, C, D, T_i)$ are the thermal conductivities calculated according to Eq. (1) with the relaxation time given by Eq. (3). The minimum of the function ($\sigma(A, B, C, D)$) gave good agreement between the calculated values and the experimental values for $\kappa(T)$, the deviation being less than the experimental inaccuracy of about 2%. Both the

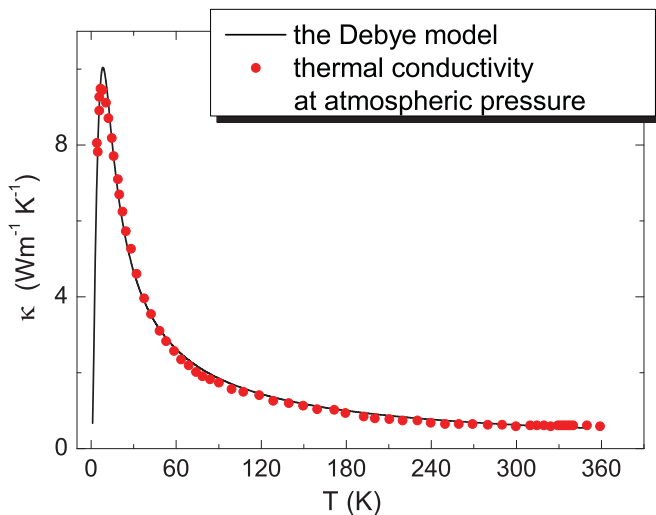


FIG. 4. (Color online) Thermal conductivity plotted against temperature at atmospheric pressure for a single crystal of $\text{Sn}_2\text{P}_2\text{S}_6$.¹⁷ The solid line represents a fit of Eq. (1) to the experimental data.

results for κ obtained here at high pressure and those of a previous atmospheric-pressure study¹⁷ were analyzed in terms of Eq. (1).

Figure 4 shows previous results for $\kappa(T)$ in the ferroelectric phase of an $\text{Sn}_2\text{P}_2\text{S}_6$ single crystal, which were measured along the [100] axis at atmospheric pressure,¹⁷ together with $\kappa(T)$ calculated by Eq. (1) using the (fitting) parameters $A = 5.2 \times 10^{-42} \text{ s}^3$, $B = 0.37 \times 10^8 \text{ s}^{-1}$, $C = 20 \text{ K}$, $D = 1.63 \times 10^{-17} \text{ s/K}$, and a value for the sound velocity (3500 m/s) of a $\text{Sn}_2\text{P}_2\text{S}_6$ monocrystal.²⁰ To qualitatively assess the relative contributions of the scattering processes (i), (ii), and (iii), we note that dominance by three-phonon Umklapp scattering gives a $\kappa \sim T^{-1}$ dependence near and above the Debye temperature, which gradually changes to an even stronger exponential dependence as the scattering freezes out at low temperature.¹¹ As the inverse point defect scattering time varies strongly with phonon frequency, this type of scattering also becomes less efficient at very low temperatures, whereas dominance by boundary scattering gives a constant phonon mean-free path, and in such cases the temperature dependence of κ is governed mostly by the variation in heat capacity. Thus, $\kappa(T)$ (Fig. 4) shows that Umklapp scattering is dominant near the Debye temperature, boundary scattering is dominant at low temperatures near the maximum in κ and below, whereas point defect scattering is important in the intermediate range (near the maximum in κ up to θ). The latter is revealed by a calculation of the thermal resistivity through Eq. (1) that includes only boundary and Umklapp scattering.

The same analysis was done for the results of the ferroelectric phase of polycrystalline $\text{Sn}_2\text{P}_2\text{S}_6$ under pressure to investigate the changes of the parameters. Since changes associated with the PT apparently affect $\kappa(T)$ well below the deduced phase line (Fig. 3), only data up to 280 K at 0.1 GPa were included in the fitting procedure. Moreover, although the weak $\kappa(T)$ of the paraelectric phase can be roughly described by Eq. (1), this would not provide any further insight in the origin of the additional phonon scattering

mechanism. Therefore, only the data of the ferroelectric phase were evaluated.

The corresponding analysis of isobaric data for κ of the ferroelectric phase at 0.1 GPa resulted in the following values: $A = 8.2 \times 10^{-42} \text{ s}^3$, $B = 1.7 \times 10^8 \text{ s}^{-1}$, $C = 39 \text{ K}$, and $D = 1.93 \times 10^{-17} \text{ s/K}$. These values suggest that scattering by U processes dominate but that point-defect scattering also gives a small contribution to the thermal resistivity in the 140–280 K range at 0.1 GPa. A comparison between these parameters for a polycrystalline sample and those of the single crystal indicate that phonon scattering at point defects and sample boundaries increase in the polycrystalline material. But in the temperature range studied here, only the former change can be regarded as reliable. Such an increase in defect scattering may arise from the large amount impurity atoms and broken bonds in the intergrain boundaries and the under-surface layers of polycrystalline semiconductors.²¹ We note that extrapolation of κ for polycrystalline $\text{Sn}_2\text{P}_2\text{S}_6$ to atmospheric pressure shows that it is slightly lower ($\sim 10\%$) than that obtained for an $\text{Sn}_2\text{P}_2\text{S}_6$ single crystal.¹⁷ This is consistent with more structural defects in the polycrystalline sample.

We turn now to consider the effect of pressure on the lattice anharmonicity. In principle, it may be possible to evaluate the change of anharmonicity through the anharmonicity-dependent parameters in Eq. (3) (e.g., D). Anharmonicity-induced phonon scattering such as U processes depends, of course, on the anharmonicity, which is reflected in the parameters. But because of the limited temperature interval and changes in other parameters such as the Debye temperature and phonon velocity, these calculations do not provide an explicit answer about the pressure-induced change of the fitted parameters. Therefore, to analyze the anharmonicity in the phases of $\text{Sn}_2\text{P}_2\text{S}_6$ we use instead data for $\kappa(p)$.

Figure 2 shows the isothermal pressure dependence of κ at 200, 263, 294, and 347 K. The rather distinct change from decreasing to increasing $\kappa(p)$ occurs at the phase boundary between the ferroelectric and paraelectric or incommensurate phases. That is, in the paraelectric and incommensurate phases, κ of $\text{Sn}_2\text{P}_2\text{S}_6$ increases with pressure, and this is consistent with the normal behavior of $\kappa(p)$ (see, e.g., Refs. 7 and 22). In the ferroelectric phase, however, $\kappa(p)$ shows an abnormal behavior as κ decreases with pressure. Only a few phases have been found to show such pressure dependence and three of those are ice phases: hexagonal ice, cubic ice, and low-density amorphous ice.⁷ In these cases, it has been confidently linked with a negative Grüneisen parameter.²³

The volume dependence of κ is conveniently described by the Bridgman parameter g ,²² which is expressed via the experimentally determined $\kappa(p)$:

$$g = - \left(\frac{\partial \ln \kappa}{\partial \ln V} \right)_T = B_T \left(\frac{\partial \ln \kappa}{\partial p} \right)_T, \quad (5)$$

where B_T is the isothermal bulk modulus and V is the volume. On the basis of the isothermal $\kappa(p)$ (shown in Fig. 2) and data for the bulk modulus of $\text{Sn}_2\text{P}_2\text{S}_6$,²⁴ we have calculated g as a function of pressure at 200, 263, 294, and 347 K using Eq. (5). The results show that the values of g range from -0.6 to -3.8 in the ferroelectric phase and from 7.2 to 9.7 in the paraelectric phase. Moreover, the most negative values for g occur near the

PT, which indicates that these are closely associated with the PT and that g may even become positive at low temperatures and low pressures.

The Bridgman parameter may also be estimated on the basis of theory for κ :²⁵

$$g = 3\gamma + 2q - \frac{1}{3}, \quad (6)$$

where $\gamma = -(\partial \ln \theta / \partial \ln V)_T$ is the Grüneisen parameter and $q = (\partial \ln \gamma / \partial \ln V)_T$ is the volume dependence of γ . For $T > \theta$ the value of q is determined by the expression²⁶

$$q = \gamma[1 + 3\alpha(B'_S - 1)T], \quad (7)$$

where α is the linear thermal expansion coefficient and B'_S is the pressure derivative of the adiabatic bulk modulus. In the temperature and pressure ranges under study, the average value of α for the ferroelectric phase of $\text{Sn}_2\text{P}_2\text{S}_6$ decreases from 1×10^{-6} to $-60 \times 10^{-6} \text{ K}^{-1}$ (approaching the PT), while in the paraelectric phase $\alpha = 20 \times 10^{-6} \text{ K}^{-1}$.²⁷ Results for the bulk modulus²⁴ give maximal values for the derivative B'_S in the range 200 to 300 near the PT; that is, even in the vicinity of the PT where B'_S is anomalously large, $3\alpha(B'_S - 1)T \ll 1$ and thus $q \approx \gamma$. It follows that Eq. (6) can be written as

$$g = 5\gamma - \frac{1}{3}. \quad (8)$$

Our results for g can now be used in Eq. (8) to calculate the Grüneisen parameter for the phases of $\text{Sn}_2\text{P}_2\text{S}_6$. Figure 5 shows the results for γ at different temperatures and pressures. Within the temperature ($T > 200 \text{ K}$) and pressure ($0.1 \text{ GPa} < p < 0.7 \text{ GPa}$) intervals under study, γ is negative in the ferroelectric phase and becomes increasingly negative approaching the PT. Thus, as for the ice phases, the abnormal decrease of κ with increasing pressure is accompanied by negative values for the Grüneisen parameter. The Grüneisen parameter decreases with pressure within the entire temperature range under study but, at the PT, it changes sign. In the paraelectric and commensurate phases γ also shows a tendency to increase with temperature. In light of these results and those reported previously for ice,²³ it is reasonable to attribute the anomalous $\kappa(p)$ of the ferroelectric phase to the negative Grüneisen parameter.

The connection between the decreasing $\kappa(p)$ and the negative Grüneisen parameter can also be discussed directly in terms of theory that considers only phonon-phonon scattering. The Grüneisen parameter calculated from values for $\kappa(p)$ should pertain to the modes responsible for the major part of the heat transport, which are typically the acoustic modes. A physical consequence of a negative Grüneisen parameter is a pressure-induced mode softening or, equivalently, a decrease of the characteristic mode frequency with increasing pressure. This causes a decrease of the Debye temperature and phonon velocity of the mode. Moreover, as shown here, at temperatures above $\sim 100 \text{ K}$, the thermal resistivity is mainly due to three-phonon U processes, and these depend on the anharmonicity. The dependence can be described in terms of the Grüneisen parameter via the parameter D in Eq. (3), which varies as $D \propto \gamma^{21,28}$ (i.e., an increasing magnitude of γ promotes U processes). In fact, when only three-phonon processes are considered, various previous estimates give $\kappa \propto V^{1/3}\theta^3/(\gamma^2T)$,¹¹ which also leads to Eq. (6). Thus, since pressurization of the ferroelectric phase causes a decrease of the Debye temperature (and phonon velocity), and the Grüneisen parameter becomes increasingly more negative, κ decreases.

Besides the implications mentioned above, there are several others associated with a negative Grüneisen parameter. The thermodynamic Grüneisen parameter, which is defined by $VB_S C_p^{-1} \alpha / 3$, where C_p is the heat capacity, is negative only when the thermal expansion is negative. This is indeed the case for $\text{Sn}_2\text{P}_2\text{S}_6$ above $\sim 200 \text{ K}$ and up the ferro- to paraelectric PT, which has been explained by the electrostriction interaction.²⁹ The negative values calculated here from $\kappa(p)$ pertain to the modes that govern the change in κ , which are normally the acoustic modes. A negative Grüneisen parameter for the (low-frequency) acoustic modes implies a negative thermal expansion coefficient at low temperatures, and there are a few such examples (e.g., ZrW_2O_8 and ice). In the latter case, the thermal expansion coefficient is positive above 73 K , but negative below this temperature,³⁰ which is consistent with the negative Grüneisen parameter derived from $\kappa(p)$ or the sound velocity.²³ Thus, the Grüneisen parameter obtained here from data for $\kappa(p)$ may seem incompatible with results

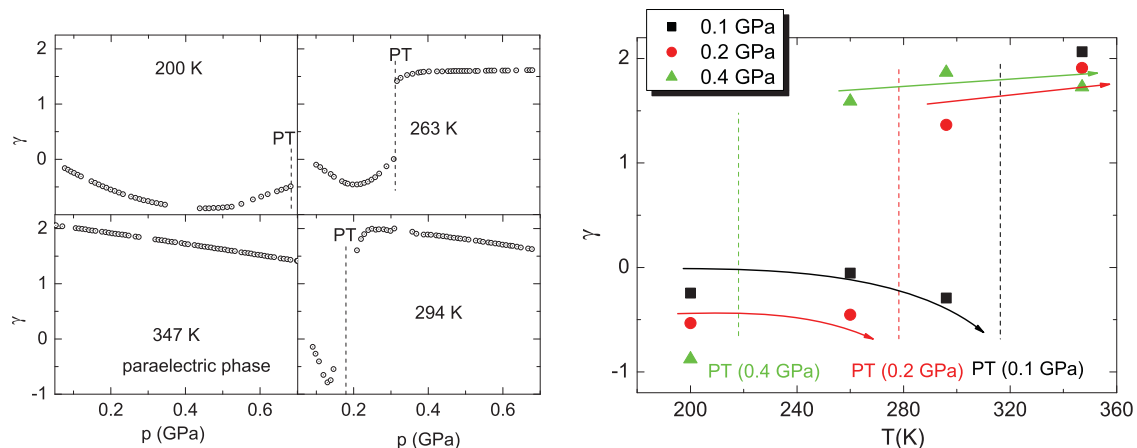


FIG. 5. (Color online) The Grüneisen parameter (γ) plotted against pressure (a) and temperature (b). The temperatures (a) and pressures (b) at which the values were calculated are indicated. Vertical dashed lines indicate the phase transition.

for the thermal expansion of $\text{Sn}_2\text{P}_2\text{S}_6$, which is positive in the range 5 to 200 K,¹ and negative from 200 K up to the PT. We find four possible explanations for these results: (a) optical modes provide the most substantial contribution to κ above 200 K, which is the lowest isotherm studied here, (b) the pressure-induced decrease of κ is caused by increased phonon scattering due to softening of optical phonons, (c) the acoustic modes softens with increasing pressure, but only near the PT due to the electrostriction interaction associated with the gradual structural change, and (d) the thermal expansion of $\text{Sn}_2\text{P}_2\text{S}_6$ is negative also at low temperatures [i.e., below the range that has been studied (<5 K)].

The first two possibilities (a) and (b) imply that the optical phonons govern the change in κ , either because of their contribution (a) or due to scattering of acoustic phonons (b). Optical modes do not normally dominate heat transport because of low velocity of optical phonons, and only (b) remains as a realistic possibility. Moreover, it would be an odd occurrence if the thermal expansivity becomes negative also at low temperatures and the temperature range up to only 5 K seems too limited to explain the size of the negative γ , which leaves (b) and (c) as the most likely explanations. As discussed above, measurements show significant changes in optical and acoustic modes approaching PT upon increasing temperature,¹⁶ which is consistent with both (b) and (c). However, the longitudinal sound velocity decreases with increasing pressure, at least in the vicinity of the PT³¹ and the transverse sound velocity also decreases strongly in the vicinity of the PT upon heating.³² Based on these results, we deduce that the unusual negative pressure dependence of κ is due mainly to pressure-induced softening of the acoustic modes caused by the gradual structural change.

Mode softening to the extent that κ decreases upon pressure increase is a relatively unusual occurrence. It has been observed for three ice phases,⁷ ammonium halides (NH_4F and NH_4Br)^{33,34}, CuCl ,³³ and possibly a few more phases. In the case of the ice phases, this feature has been studied by pressurization at low temperatures below 140 K where crystal-crystal transitions in ice are kinetically hindered. In all three ice phases, pressurization causes the lattice to collapse to an amorphous state, which has been attributed to the Born instability.³⁵ Thus, the unusual $\kappa(p)$ of the ferroelectric phase of $\text{Sn}_2\text{P}_2\text{S}_6$, which is linked to a negative Grüneisen parameter or mode softening indicates that $\text{Sn}_2\text{P}_2\text{S}_6$ may also collapse to an amorphous state upon compression at low temperatures. Kinetic hindrance of a second-order transition, which here is a requirement for a collapse to an amorphous state, is a less likely occurrence than that of a first-order transition with significant structural rearrangement. But since the transition

gradually changes from a second-order to a first-order type of transition with decreasing temperature,³ pressure-induced amorphization of the $\text{Sn}_2\text{P}_2\text{S}_6$ ferroelectric phase may occur upon pressurization at low temperatures.

IV. CONCLUSIONS

The thermal conductivity of the ferroelectric, paraelectric, and incommensurate phases of polycrystalline $\text{Sn}_2\text{P}_2\text{S}_6$ has been measured in the temperature range from 140 to 370 K for pressures up to 0.7 GPa. On the basis of the isothermal and isobaric dependencies, we have analyzed the phonon scattering mechanisms and the temperature and pressure behaviors of the anharmonicity in $\text{Sn}_2\text{P}_2\text{S}_6$. The analysis of the temperature behavior of the ferroelectric phase, which was made within the framework of the Debye model, indicates that phonon-phonon scattering and scattering by sample defects and boundaries are the main mechanisms for thermal resistivity. Near and above the ferroelectric to paraelectric or incommensurate phase transition, the thermal conductivity becomes temperature independent, and the latter two phases cannot be distinguished on the basis of their thermal conductivities. The weak temperature dependence of the thermal conductivity, which is generally associated with glasses and other amorphous states, has previously been observed in relatively few normal crystal phases. In $\text{Sn}_2\text{P}_2\text{S}_6$, it arises near the ferro- to paraelectric (or incommensurate) displacive type of phase transition, which is accompanied by softening of optical phonons that can promote phonon-phonon scattering processes, but the detailed reason for the glasslike behavior of the thermal conductivity for $\text{Sn}_2\text{P}_2\text{S}_6$ and other crystal phases remains obscure.

The abnormal pressure-induced decrease of the thermal conductivity for the ferroelectric phase is confidently linked to a negative Grüneisen parameter, and it becomes increasingly more negative as the phase transition boundary is approached by increasing pressure and/or temperature. A decrease of thermal conductivity upon pressurization has previously been observed for only a few other phases of which several collapse to an amorphous state, which indicates that this may also occur for $\text{Sn}_2\text{P}_2\text{S}_6$ at low temperatures where crystal-crystal transitions are kinetically hindered.

Finally, we note that $\text{Sn}_2\text{P}_2\text{S}_6$ seems to be a unique crystal, which shows both glass-like temperature dependence and negative isothermal pressure dependence for the thermal conductivity. This combination of rarely observed thermal conductivity behaviors calls for further detailed investigations of the phonon properties of the ferroelectric phase under pressure, especially since the origin of the glass-like thermal conductivity of crystals is yet to be firmly established.

¹D. G. Semak, V. M. Rizak, and I. M. Rizak, *Photothermostructural Transformation of Chalcogenides* (Zakarpatyya, Uzhhorod, Ukrainian, 1999).

²Yu. M. Vysochanskii, T. Janssen, R. Currat, R. Folk, J. Banys, J. Grigas, and V. Samulionis, *Phase Transitions in Phosphorous Chalcogenide Ferroelectrics* (Vilnius University, Vilnius, 2006).

³Yu. I. Tyagur and E. I. Gerzanich, *Sov. Phys. Crystallogr.* **29**, 563 (1984).

⁴O. Andersson, O. Chobal, I. Rizak, and V. Rizak. *Phys. Rev. B* **80**, 174107 (2009).

⁵S. Stølen and T. Grande, *Chemical Thermodynamics of Materials: Macroscopic and Microscopic Aspects* (Wiley, New York, 2003).

- ⁶B. Håkansson, P. Andersson, and G. Bäckström, *Rev. Sci. Instrum.* **59**, 2269 (1988).
- ⁷O. Andersson and A. Inaba, *Phys. Chem. Chem. Phys.* **7**, 1441 (2005).
- ⁸C. D. Carpentier and R. Nitsche, *Mater. Res. Bull.* **9**, 401 (1974).
- ⁹R. G. Ross and O. Sandberg, *J. Phys. C* **12**, 3649 (1979).
- ¹⁰B. Scott, M. Pressprich, R. D. Willet, and D. A. Cleary, *J. Solid State Chem.* **96**, 294 (1992).
- ¹¹R. Berman, *Thermal Conduction in Solids* (Clarendon, Oxford, (1976).
- ¹²O. Andersson, R. G. Ross, and R. G. G. Bäckström, *Mol. Phys.* **66**, 619 (1989).
- ¹³M. M. Koza, M. R. Johnson, R. Viennois, H. Mutka, L. Girard, and D. Ravot, *Nat. Mater.* **7**, 805 (2008).
- ¹⁴M. Tachibana, N. Taira, H. Kawaji, and E. Takayama-Muromachi, *Phys. Rev B* **82**, 054108 (2010).
- ¹⁵M. W. C. Dharma-Wardana, *J. Phys. Chem.* **87**, 4185 (1983).
- ¹⁶S. W. H. Eijt, R. Currat, J. E. Lorenzo, P. Saint-Grégoire, B. Hennion, and Yu. M. Vysochanskii, *Eur. Phys. J. B* **5**, 169 (1998).
- ¹⁷V. M. Rizak, K. Al'-Shoufi, I. M. Rizak, I. P. Prits, Yu. M. Vysochanskii, and V. Yu. Slivka, *Ferroelectrics* **155**, 323 (1994).
- ¹⁸V. Rizak, A. Bokotey, I. Rizak, K. Al'-Shoufi, and V. Slivka, *Ferroelectrics* **192**, 149 (1997).
- ¹⁹J. E. Parrot and A. D. Stuckes, *Thermal Conductivity of Solids* (Pion Limited, London, 1975).
- ²⁰V. Valevichius, V. Samulionis, and V. Skritskij, *Ferroelectrics* **79**, 225 (1988).
- ²¹J. P. Suhet, *Chemical Physics of Semiconductors* (Van Nostrand, London, 1965).
- ²²P. W. Bridgman, *The Physics of High Pressure* (McMillan, New York, 1931).
- ²³O. Andersson and A. Inaba, *J. Chem. Phys.* **122**, 124710 (2005).
- ²⁴A. G. Slivka, E. I. Gerzanich, P. P. Guranich, V. S. Shusta, V. M. Kedyulich, *Condens. Matter Phys.* **2**, 415 (1999).
- ²⁵G. A. Slack, *Solid State Physics*, Vol. 34 (Academic Press, New York, 1979), p. 1.
- ²⁶R. Rao, *J. Phys. Soc. Jpn.* **38**, 4, 1080 (1975).
- ²⁷M. M. Maior, B. M. Koperles, and B. A. Savchenko, *Fiz. Tverd. Tela (Leningrad)* **25**, 214 (1983); *Sov. Phys. Solid State* **25**, 117 (1983).
- ²⁸J. M. Ziman, *Electrons and Phonons* (Oxford University Press, Oxford, 1960).
- ²⁹M. M. Khoma, A. A. Molnar, and Yu. Vysochanskii, *J. Phys. Stud.* **2**, 524 (1998).
- ³⁰K. Röttger, A. Endriss, J. Ihringer, S. Doyle, and W. F. Kuhs, *Acta Crystallogr. B* **50**, 644 (1994).
- ³¹Yu. M. Vysochanskii, A. A. Kohutych, A. V. Kityk, A. V. Zadorozhna, M. M. Khoma, and A. A. Grabar, *Ferroelectrics* **399**, 83 (2010).
- ³²V. D. Valevichius, V. I. Samulenis, Yu. M. Vysochanskii, M. M. Maior, and M. I. Gurzan, *Sov. Phys. Solid State* **31**, 1180 (1989).
- ³³R. G. Ross, P. Andersson, B. Sundqvist, and G. Bäckström, *Rep. Prog. Phys.* **47**, 1347 (1984).
- ³⁴R. G. Ross and O. Sandberg, *J. Phys. C* **20**, 4745 (1987).
- ³⁵M. Born and K. Huang, *Dynamic Theory of Crystal Lattices* (Clarendon, Oxford, 1954).